SUPPLEMENTARY INFORMATION:

SAXS measurements on different sample thickness :

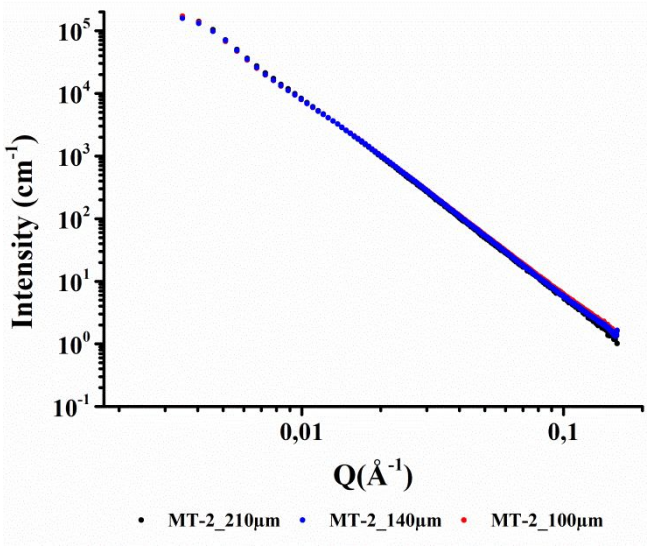

Figure SI-1. *SAXS profiles obtained on MT-2 according to three different thickness : 100 µm (red dots), 140 µm (blue dots) and 210 µm (black dots).*

HS-GC measurements along source rocks lamination

Another HS-GC experiment has led to transport properties and is represented Figure SI-2, for that BSP-4 sample was analyzed according to parallel or normal to the lamination plane. At first, the distribution of hydrocarbons remains the same within the observed plane. Then, it appears that the diffusion through the rock is higher in the case of normal to bedding plane. This illustrates, the presence of preferential pathways generated by the rock structure, especially impermeable layer associated with clay minerals.[17,36]

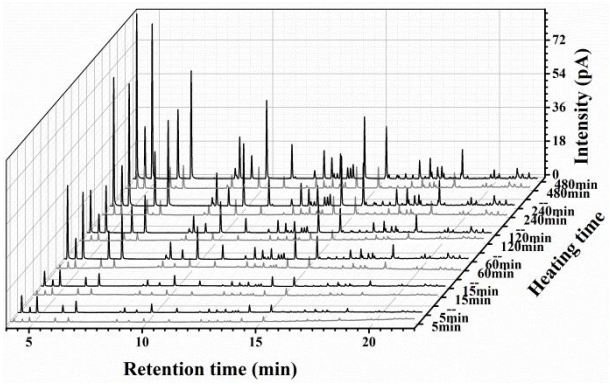

Figure SI-2. Chromatographs of the BSP-4 sample showing the diffusion through the sample of n-alkane according parallel (grey) or normal (black) to the lamination.

I(Q) as a function of lamellar mineral content

From scattering profiles, an increasing loss of intensity is remarked in Figure 10 and in Figure 11 from MT-1, BSP-2 and BSP-3 to BSP-4 and BSP-5. This loss can be expressed by the ratio $\boldsymbol{I_{para/norm}} = \frac{\boldsymbol{I(Q)\_sample\_para}}{\boldsymbol{I(Q)\_sample\_norm}}$ which is noted in Table SI-1. After comparison with the lamellar mineral content, the increase of $\boldsymbol{I_{para/norm}}$ and the quantity of layered minerals is correlated for both SAXS/WAXS and SANS profiles. It seems the higher these parameters, the lower the α parameters. This inverse correlation can be explained by the predominance of mineral phases on this Q-region.

Table SI-1. Parameters α, $I_{para/norm}$ and lamellar mineral content that defined the algebraic tendency at low Q values on SANS and SAXS/WAXS profiles.

Reference	α (SANS)	α (SAXS/WAXS)	$I_{para/norm}$ (SANS)	$I_{para/norm}$ (SAXS/WAXS)	Micas (wt %)	Clay (wt %)	Total lamellar content (wt %)
BSP-2	3.2	3.2	1.6	2.1	16.4	12.4	28.8
BSP-3	3.2	3.2	1.5	2.4	14.5	14.9	29.4
BSP-4	3.1	3.1	2.6	3.4	28.9	19.4	42.3
BSP-5	3.1	3.1	2.2	3.8	23.6	12.7	36.3
MT-1	3.4	3.4	1.0	0.9	18.0	4.2	22.2

I(Q) as a function of TOC content

These data were only used to define if the high Q region is sensitive to TOC content. In this diagram, the trend breakdown starts at 0.12 $Å^{-1}$. These variations of I(Q) seem to be relied on organic properties of the source rocks. Considering the kerogen and the porous system as homogeneous phases, the SLD contrast $\Delta\rho^2_{(P-K)}$ stay constant. Thus, I(Q) variations depend on the occurrence of pore in the Kerogen N_p and their volume fraction Φ_p. One may assume that no differences between parallel and normal to the elongation of 2D anisotropic pattern were remarked for this Q-region. As displayed in Figure SI-3, at high Q values an uprising of I(Q) is observed on φ_2 integrated azimuthal angle and appears to be linked to the TOC content of the sample. BSP-2, BSP-3 and MT-1 have a TOC content of 4.5 to 4.8 wt % and their SANS profiles are lower than BSP-4 and BSP-5 sample which have, respectively, 9.0 and 8.1 wt % of TOC.

Other variations occur from 0.1 to 0.2 Å^{-1} which can be due to a differentiation of pore size in the kerogen.

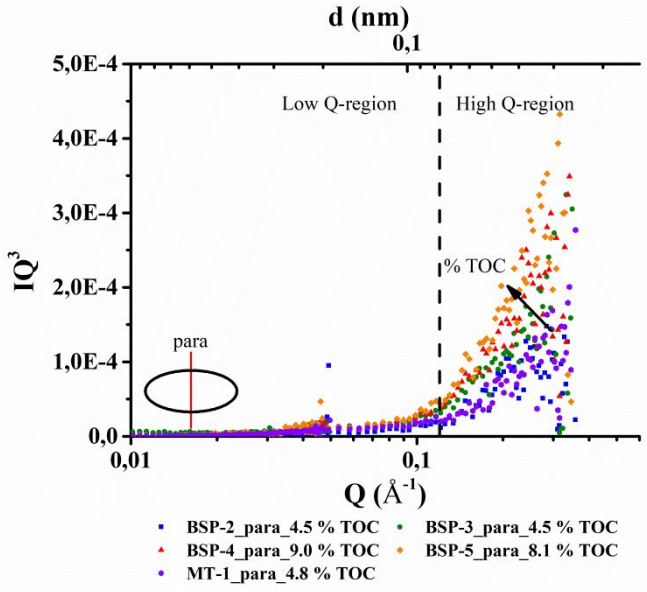

Figure SI-3. IQ^3 SANS profiles of parallel to the 2D anisotropic pattern, as a function of the scattering vector Q that reveal the relation between I(Q) and the TOC content.

Pyrite considerations on SAXS data

In the case of X-rays measurements, the fit of the mineral phases at low Q-region, assuming similar parameters as SANS fit, leads to the observation of a mismatched area. Considering the presence of pyrite, SAXS data at low Q values < 0.05 Å^{-1} are discussed as a function of pyrite content in Figure SI-4(a). After normalization to a same starting point at Q = 0.05 Å^{-1}, the decrease of intensity seems to be correlated with pyrite content. The fit of SAXS data was performed assuming pyrite ($\Delta\rho^2_{(Py-K)}$) and other minerals ($\Delta\rho^2_{(M-K)}$) contributions to the SLD contrast, as illustrated in Figure SI-4(b). For SANS, the mineral phase is assumed to be

homogeneous and its SLD contrast with Kerogen at low Q values is expressed as $\Delta\rho^2_{(M-K)}$. For high-Q values, the SLD contrast is defined by the pore to Kerogen contrast as $\Delta\rho^2_{(P-K)}$.

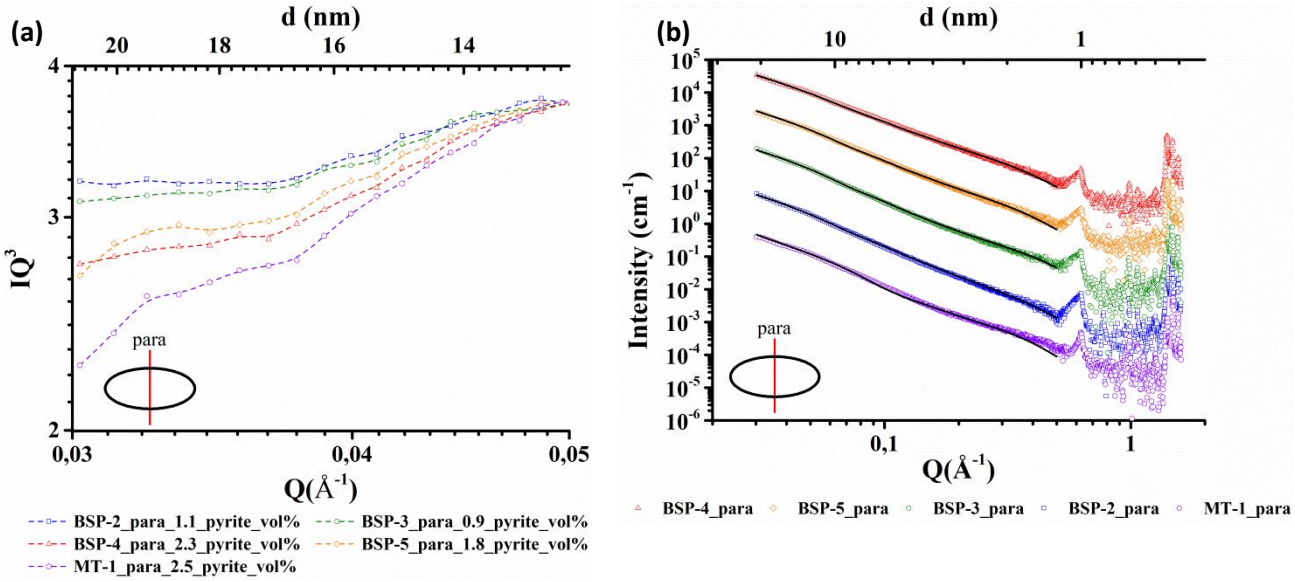

Figure SI-4. (a) SAXS profiles from area highlight in Figure 8 which are adjusted to start at the same value of Q = 0.05 Å^{-1}. Pyrite content is indicated for each sample. (b) Initial sample SAXS/WAXS and fit profiles with a correction by the addition of pyrite contribution.

Fit sensitivity

In addition, fit sensitivity on the pore size radius was tested with values ranging from 0.4 nm to 1.1 nm. After removal of fit data to far from sample data, results from BSP-2 samples are shown in Figure SI-5 and reveal an uncertainty on the pore radius size of ± 0.1 nm.

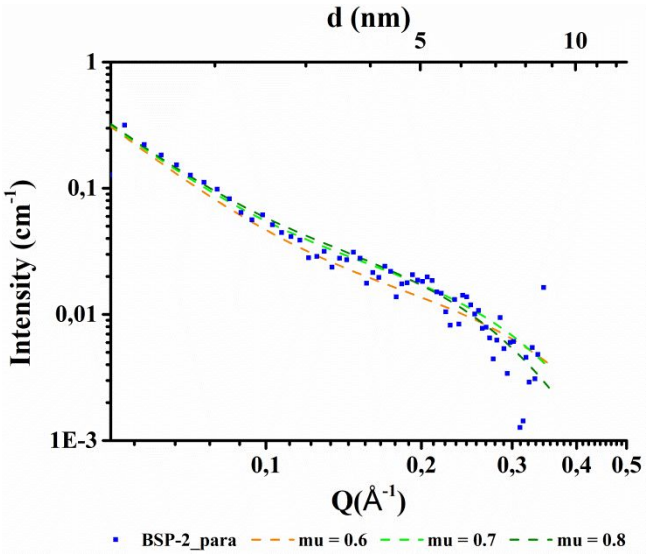

Figure SI-5. Fit sensitivity of the pore size radius fit for BSP-2 samples. Fit in dark green dash line is consistent with pore radius of 0.8, light green dash line with pore radius of 0.7 nm and orange dash line with pore radius of 0.6 nm.